Observations of Latex Particle Two-Dimensional-Crystal Nucleation in Wetting Films on Mercury, Glass, and Mica

Antony S. Dimitrov,[†,‡] Ceco D. Dushkin,[†,‡] Hideyuki Yoshimura,[‡] and Kuniaki Nagayama*[,‡]

Laboratory of Thermodynamics and Physico-chemical Hydrodynamics, Faculty of Chemistry, University of Sofia, 1126 Sofia, Bulgaria, and Nagayama Protein Array Project, ERATO, JRDC, Tsukuba Research Consortium, 5-9-1 Tokodai, Tsukuba, 300-26, Japan

Received July 12, 1993. In Final Form: November 15, 1993[⊗]

We studied the nucleation of two-dimensional crystals from micrometer- and submicrometer-size latex particles in liquid films formed on mercury, glass, and mica. For the experiments on mercury we controlled both the film thickness and the mercury surface electric potential, whereas for the experiments on glass and mica we traced the film thickness as a function of time. The nucleation of monolayers from micrometer-size particles was obtained on mercury only in a narrow interval of low positive electric potentials applied to the mercury. Both the micrometer and the submicrometer particles started to assemble when the film thickness became equal to the particle diameter. Our results suggest that the lateral capillary immersion forces, which appeared between the particles protruding from the liquid film, arranged these particles in a two-dimensional-crystal nucleus.

Introduction

Two-dimensional (2D) crystallization of latex particles on a substrate can find various applications.[1-4] The latex crystals can also model 2D arrays of protein macromolecules[5-6] and other biological species like viruses, organelles, and even cells.

The 2D crystallization strongly depends on the wettability and the smoothness of the substrate surface. Different substrates of increasing cleanliness and homogeneity were used: glass,[7,8] mica,[8] and mercury.[6] Two-dimensional protein arrays were formed on clean mercury surfaces by spreading of protein solutions.[6] Two-dimensional crystals of latex particles were also prepared on mercury by using the same method. A wetting liquid film was formed on mercury for both systems, and the crystals were obtained after the film drying. Recently Denkov et al.[7] and Dushkin et al.[8] analyzed the kinetics of 2D crystallization of latex particles on solid substrates. These researchers placed the suspension of micrometer[7] or submicrometer[8] latex particles in a crystallization cell that had a cylindrical hydrophobic inner wall (Teflon[7] or paraffin[8]) and a hydrophilic bottom (solid substrate). Then they let the water in the suspension evaporate from the cell. The cell shaped the suspension layer so that its central part was always thinner than that near the cylindrical wall. The crystal growth started in the cell center and progressed radially toward the cell periphery. Two distinct stages of the crystallization process were reported in these studies[7,8]—nucleation and crystal growth. The nucleus was a crystalline monolayer of particles with closed packing. The particles were most likely collected into the nucleus by the lateral capillary immersion forces.[9,10] The water prominently evaporated from the film surface over the formed nucleus. The particles in the nucleus prevented the film thinning, and water from the suspension in the Gibbs-Plateau border flowed into the forming nucleus to compensate for the evaporation. The water flux carried along latex particles, which attached outside to the nucleus. Thus, the crystal grew. There were some observations in refs 7 and 8 suggesting the validity of the capillary force hypothesis for the nucleus formation. However, (1) the extent of nucleation was not well clarified and (2) the most crucial parameter in the theory, the thickness of the wetting film, was not determined during the nucleus formation. Therefore, the above hypothesis has not yet been properly proven.

We studied the latex particle 2D nucleation in liquid wetting films on mercury, glass, and mica. The nucleation was examined in relation to the film thickness, which was recorded as a function of time in the experiments on mica and glass and was controlled in the experiments on mercury by suspension injecting into or withdrawing from the cell. Various electric potentials were also applied to mercury to study the 2D crystal nucleation dependence on the particle–substrate interactions.

Experimental Section

1. Materials. We used polystyrene latex beads (JSR, the original suspension concentration was 1 wt %) of different diameters (see also Table 1). The latex particles in the suspension were negatively charged (ζ potentials were −106 and −90 mV for the particles with diameters of 1696 and 814 nm, respectively).[7] The solutions were prepared from the original suspension by dilution with deionized water. Sodium dodecyl sulfate (SDS, Fisher) was used to improve the wettability of mercury. The

* To whom correspondence should be addressed.
† University of Sofia.
‡ ERATO Protein Array Project.
⊗ Abstract published in *Advance ACS Abstracts*, January 15, 1994.
(1) Alfrey, T. A.; Bradford, E. B.; Vanderhoff, J. W.; Oster, G. *J. Opt. Soc. Am.* **1954**, *44*, 603.
(2) Krieger, I. M.; O'Neill, F. M. *J. Am. Chem. Soc.* **1968**, *90*, 3114.
(3) Deckman, H. W.; Dunsmuir, J. H. *Appl. Phys. Lett.* **1982**, *41*, 377.
(4) Hayashi, S.; Kumamoto, Y.; Suzuki, T.; Hirai, T. *J. Colloid Interface Sci.* **1991**, *144*, 538.
(5) Wildhaber, I.; Gross, H.; Engel, A.; Baumeister, W. *Ultramicroscopy* **1985**, *16*, 411.
(6) Yoshimura, H.; Matsumoto, M.; Endo, S; Nagayama, K. *Ultramicroscopy* **1990**, *32*, 265.
(7) Denkov, N. D.; Velev, O. D.; Kralchevsky, P. A.; Ivanov, I. B.; Yoshimura, H.; Nagayama , K. *Langmuir* **1992**, *8*, 3183.
(8) Dushkin, C. D.; Yoshimura, H.; Nagayama, K. *Chem. Phys. Lett.* **1993**, *204*, 455.
(9) Kralchevsky, P. A.; Paunov, V. N.; Ivanov, I. B.; Nagayama, K. *J. Colloid Interface Sci.* **1992**, *151*, 79.
(10) Kralchevsky, P. A.; Paunov, V. N.; Denkov, N. D.; Ivanov, I. B. Nagayama, K. *J. Colloid Interface Sci.* **1992**, *155*, 420.

0743-7463/94/2410-0432$04.50/0 © 1994 American Chemical Society

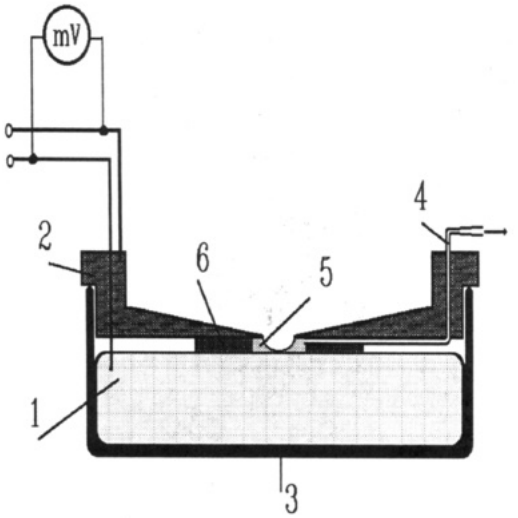

Figure 1. Experimental cell for preparation of latex arrays on mercury: (1) mercury, (2) bronze cover, (3) container for mercury, (4) syringe needle, (5) latex suspension, (6) plastic ring (cell wall).

Table 1. Specifications of the Latex Particles Given by the Producer

latex code	diameter (nm)	polydispersity (nm)	density (g/cm^3)	particle refractive index
SC-171-S	1696	± 47	1.057	1.592
SC-081-S	814	± 23	1.065	1.565
SC-015-S	144	± 2	1.065	1.565
SC-005-R	55	± 3.6	1.065	1.565

mercury was of high purity (99.9999%, Mitsuwa's Pure Chemicals). Matsunami microcovers were used as glass substrates. Mica substrates were freshly cleaved on both sides. Paraffin blocks (20 × 10 × 5 mm) with a melting point of about 70 °C were used for preparation of the cells, which were used for studying the nucleation on glass and mica.

2. Experimental Cells and Apparatus. The experimental cell for particle monolayer nucleation on mercury is shown in Figure 1. Mercury (part 1 in Figure 1) is in a 5-cm-diameter glass container (part 3). The cell cover (part 2) is made of bronze to conduct electricity (we used the cover as a reference electrode for mercury polarization). The cell wall (part 6) is a plastic ring with a 1-cm inner diameter and a 0.1-cm thickness. The ring is glued to the bronze cover so that it lightly touches the mercury surface and restricts the volume of the solution, which was being investigated. The syringe needle (part 4) piercing the plastic wall allows for a control of the suspension volume inside the cell and, therefore, for a control of the suspension layer thickness. Two electrical wires are attached to the bronze cover and to the mercury. Thus, the electric potential applied to the mercury can be varied.[11,12] The potential difference between the mercury and the cell cover is measured by a millivoltmeter.

The details of the crystallization cells for growing 2D crystals of submicrometer latex particles on solid substrates are given in ref 8. The cells were circular holes with diameters of 2 mm in paraffin blocks of 20 × 10 × 5 mm size. These blocks were sealed to the substrates (glass or mica) by melting the paraffin surface. Thus, the cells had hydrophobic walls and hydrophilic bottoms as substrates.

The particle nucleation on mercury was observed by a differential interference optical microscope (Epival Interfako, Carl Zeiss, Jena) equipped with 25× and 12.5× objectives with numerical apertures of 0.5 and 0.25, respectively. The light source was a high-pressure mercury lamp (HBO-50, Germany) combined with a filter transmitting only the green spectral line with a wavelength of 546 nm.

The nucleation on glass and mica substrates was observed by an Olympus (Japan) optical microscope in reflected light equipped with an objective of 10× with a numerical aperture of 0.30. The light source was a halogen lamp combined with a filter transmitting the light with a wavelength of 546 nm. The obtained nucleus structure was studied by using a scanning electron microscope (SEM JSM820, JEOL) and a transmission electron microscope (TEM JEM1200 EX-II, JEOL).

The nucleation process on both mercury and solid substrates was recorded with a video camera recorder. The radii of the interference fringes were measured from a TV monitor by using an image analyzer (Zeiss Videoplan 2).

3. Experimental Conditions and Procedures. All our experiments were carried out at room temperature, 20–21 °C, and a humidity of 30–70%.

We washed commercial (or distilled) mercury with 10% nitric acid and rinsed it with deionized water until the waste water became neutral (about pH 7). If impurities persisted after this washing procedure, they would be attached to the mercury surface. To avoid the transfer of such surface impurities into the experimental cell, we used a clean polyethylene syringe to withdraw pure mercury from deep within the washed mercury and injected this into the cell.

For an easier wetting of the mercury in the cell, an aqueous solution of 0.01 mol/L sodium dodecyl sulfate and 0.15 mol/L NaCl was used. A negative potential of −200 mV was also applied to the mercury in the beginning of each experiment. The bare mercury surface in the experimental cell quickly (within 2–3 s) adsorbed gases (especially water vapors) from the atmosphere. The solution dropped on this mercury surface did not spread and formed drops moving on the surface. The drops accumulated near the cell wall when they touched the cell cover, and a bare circular surface of mercury remained in the cell center. We withdrew mercury from above in the center of this spot. When this was done, adsorbed materials were also removed along with the mercury. The newly created mercury surface was wettable by the solution, and a wetting film was formed on the mercury. We kept the applied negative potential on mercury at least for half an hour, while the sodium dodecyl sulfate molecules, which were in the solution, adsorbed onto the mercury/water interface, thus decreasing the interfacial tension and stabilizing the formed wetting film. After forming a stable wetting film on the mercury surface, we withdrew as much of the bulk-phase solution from the cell as was possible and washed the mercury surface three times with deionized water. We kept the water in the cell for no more than 10 s each time in order to remove the sodium chloride from the cell, but to hold the adsorbed monolayer of SDS molecules on the mercury. After washing we put 2 or 3 droplets of the latex suspension into the experimental cell and changed the potential that we applied to the mercury to the value that was kept during the nucleation. The thickness of the suspension layer, thus formed, was much above 10 μm. (This layer was not transparent for the microscope, and its thickness was not measured. Simple calculations using the droplet volume showed that it should be around 500 μm.) The obtained thick film was made thinner by withdrawing suspension from the cell

(11) Matsumoto, M.; Montandon, C.; Hartland, S.; Watanabe, A. *Chem. Eng. Sci.* **1978**, *33*, 831.
(12) Kaisheva, M. *Adv. Colloid Interface Sci.* **1992**, *38*, 319.

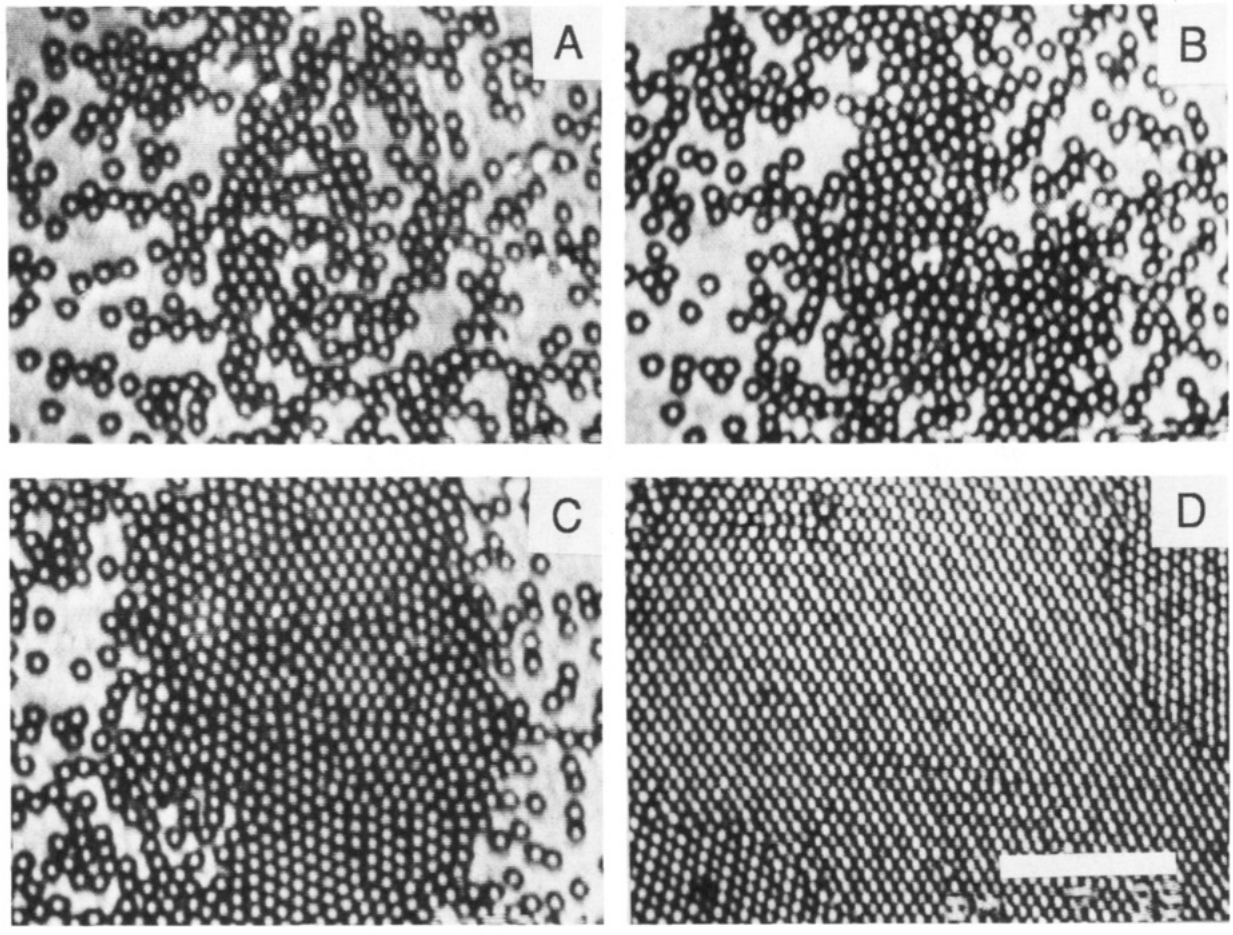

Figure 2. Nucleation of 1696-nm latex particles on mercury: (A) start of the nucleation, the particles associate in clusters, time t at that moment is set as zero; (B) increase in the number of clusters (t = 1 min); (C) transition to ordered assembly with a hexagonal structure (t = 4 min), slight directional motion of particles toward the assembly was observed; (D) improving of the nucleus structure. The bar corresponds to 20 μm.

through the syringe shown in Figure 1. When the film was made thinner, water flowed from its center toward the surrounding bulk suspension. The water flow carried along latex particles and decreased their number in the film. To prevent particle depletion in the film, we decreased the rate of withdrawal when the film thickness became less than 10 μm. Then the film continued to become thin due to the water evaporation. When the upper film surface pressed the particles lightly to the substrate, the film thickness was kept constant by carefully injecting the suspension into the cell and an ordered nucleus formed.

The experimental procedures on glass and mica were much simpler. The cell was loaded with a 1 μL suspension of latex particles with 0.05–0.1% particle weight concentration. Then the water was allowed to evaporate freely. No withdrawal or injection of liquid was done. The film thickness was recorded as a function of time. The dried 2D-crystal samples for SEM analysis were coated first with carbon and then with a gold layer (about 5-nm thicknesses) by vacuum evaporation. For the TEM analyses, the 2D crystals on the mica sheet were coated with a carbon film and the carbon film together with the 2D crystals was removed from the mica by floating these at the water surface.

4. Film Thickness Measurements. We measured suspension film thicknesses from 2 to 10 μm with an accuracy of $\pm$0.5 μm by successively focusing the microscope at the mercury and water surfaces. Thicknesses of less than 2 μm were computed from the interference pattern (see the Appendix).

Results

1. Micrometer-Size Particles. With these particles we observed *in situ* the behavior of the particles in the suspension film when different electric potentials were applied to the mercury. In the next four paragraphs we describe the results, which were obtained for four different types of electric potentials applied to the mercury.

When a negative potential was applied to the mercury surface (about 200 mV or more), the latex particles floated up, and after reaching the upper layer surface, hexagonal-ordered domains appeared. When the suspension was withdrawn from the cell, these domains disappeared and the latex particles were carried along by the water flux into the Gibbs–Plateau border.

When a negative potential of less than 200 mV was applied to the mercury, the latex particles remained in the suspension until the film surface pressed them to the mercury. Then the latex particles escaped the film, and a particle-free film was formed.

When a positive potential was applied to the mercury surface (about 100 mV or more), the latex particles sedimented and became strongly attached to the mercury surface, thus forming bumps and open places. In the open places the film was usually ruptured. The three-phase contact line, which was formed between mercury, suspension, and air, expanded toward the cell periphery and carried the particles back to the bulk suspension.

We observed the nucleation of a 2D crystallization when a low positive potential, between 3 and 10 mV, was applied to the mercury. In this range of applied potentials the

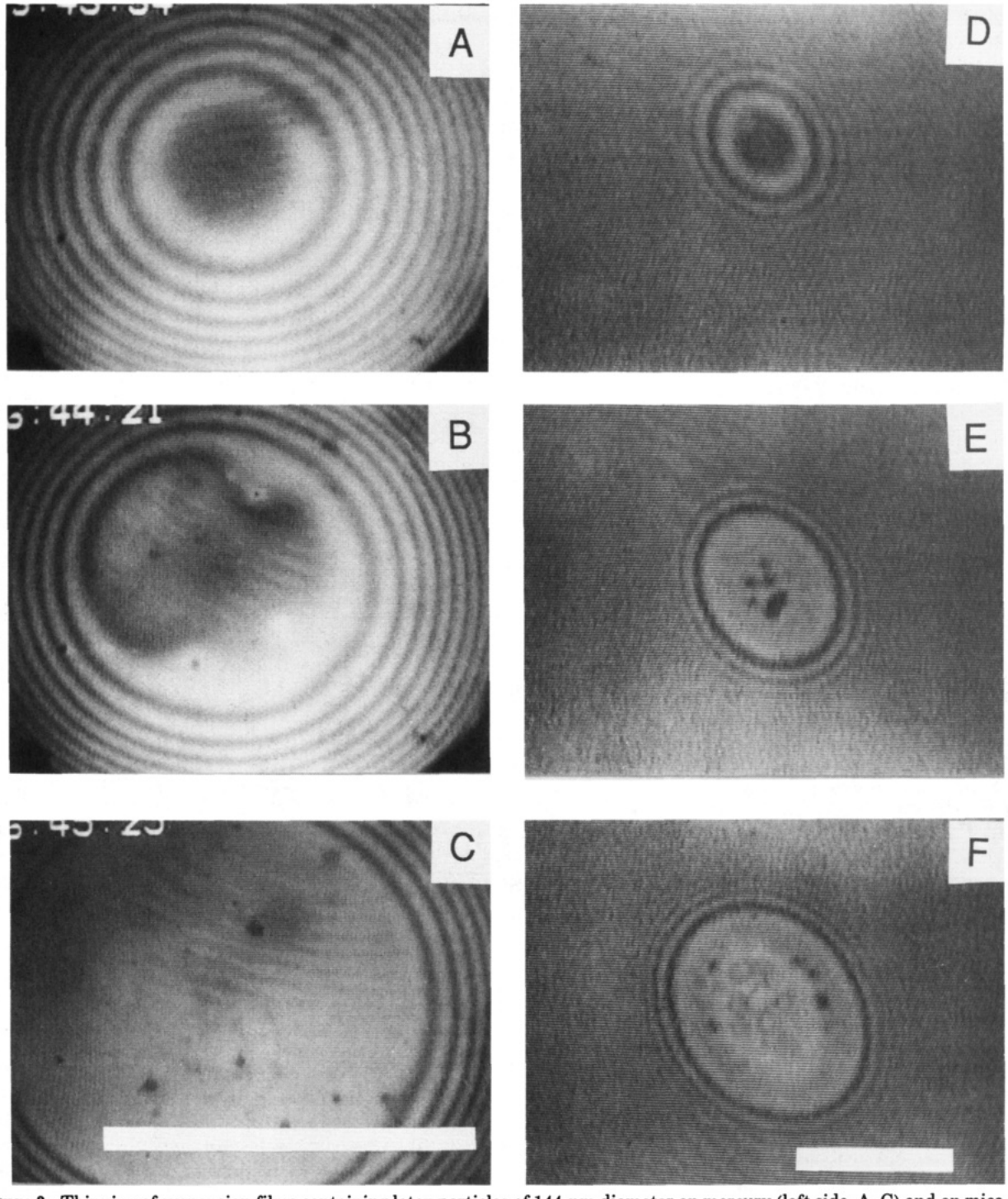

Figure 3. Thinning of suspension films containing latex particles of 144-nm diameter on mercury (left side, A–C) and on mica (right side, D–F): (A) appearance of Newton rings (t = 0 s); (B) formation of a thin liquid film of thickness $h \approx 200$ nm (t = 45 s) on mercury; (C) nucleus formed in the thin liquid film of thickness $h \approx 148 \pm 20$ nm (t = 85 s) on mercury; (D) Newton rings from the film on mica (t = 0 s); (E) dark spots in the film on mica ($h \approx 160 \pm 20$ nm, t = 9 s) at the beginning of the nucleation; (F) final steps of the nucleation on mica ($h \approx 155 \pm 20$ nm, t = 17 s). The bars are 150 μm each.

wetting film containing latex particles was stable, the particles did not make bumps on the mercury surface, and they remained inside the film instead of going into the Gibbs–Plateau border when the film surface pressed them to the mercury. The nucleation process started when the film thickness became nearly equal to the particle diameter. This is illustrated in Figure 2 for particles with diameters of 1696 nm. Initially, the latex spheres were seen to have Brownian motion. When this motion became slightly localized, we stopped the film thinning process by carefully injecting suspension into the cell. At the beginning of the crystalline-monolayer nucleation, the particle density in the film slightly increased (middle part of Figure 2A) and the particles that were closer to each other aggregated. Oppositely, the particles that were located apart from each other distanced more. The behavior of the particles at this first step of the nucleus formation led to a redistribution of the particle density in the film. The particles in the places with high particle density then associated into clusters. At the second step of the formation of a crystalline-monolayer nucleus, the areas of the clusters increased gradually (Figure 2B) and the clusters joined together (Figure 2C). Then the unidirectional speed of the particles toward the 2D array

was visually observed to increase. Therefore, the particle motion caused by the evaporation of water surpassed the particle motion due to the lateral immersion capillary forces, and it can be inferred that the nucleus was already formed. The ordered 2D nucleus had an average diameter of about 60 μm. Further, some defects in the nucleus structure disappeared during the crystalline-monolayer growth. After the nucleation was finished, the annealing of the nucleus structure proceeded in the third step of the nucleus formation. Finally, the nucleus was well packed in a 2D hexagonal lattice (Figure 2D).

Similar experiments were also done with latex particles with diameters of 814 nm. The nucleation was as that described above for the larger particles. The only difference was that the Brownian motion was faster and nuclei were formed even at low negative potential (up to 10 mV) applied to the mercury.

2. Submicrometer-Size Particles. We consider below the nucleation of 2D crystals from latex particles with diameters of 144 nm and latex particles with diameters of 55 nm. Figure 3 represents the thinning process of the film containing 144-nm latex particles on mercury (left side) and on mica (right side).

On mercury we withdrew suspension relatively quickly from the cell until well-defined Newton rings appeared in the cell center (Figure 3A). A plane-parallel film began to form when the film thickness was about 200 nm (Figure 3B). We carefully started to decrease the film thickness by withdrawing the suspension from the cell through the syringe piercing the cell wall (Figure 1). The contact line was expanded little during this process. Finally, the film thickness became almost equal to the particle diameter (Figure 3C), and the monolayer nucleus was formed. The film thickness was calculated to be 148 ± 20 nm without correction for the particle concentration as it is written at the end of the Appendix. After formation of the monolayer nucleus, shown in Figure 3C, the contact line was expanded by a controlled increase of the capillary pressure (by withdrawing suspension from the cell), but the calculated film thickness did not decrease. The 2D crystal continued to grow.

Three stages of the suspension film thinning process on the mica surface are shown on the right side of Figure 3. About half an hour after loading the cell, the suspension layer on the mica surface became thin enough and interference Newton rings appeared (Figure 3D). After 5–10 s a plane-parallel thin liquid film was formed (Figure 3E). The film–meniscus contact line had a mean radius of about 100 μm. When the film thickness ($h \approx 157$ nm, without correction) became almost equal to the particle diameter, several dark spots appeared simultaneously inside the film. With this, we supposed that the nucleation was completed. The spots did not contain particles. They represented concave water films with thicknesses of about 100 nm, which is much less than the particle diameter. The spots became bright after drying of the nucleus (central part in Figure 3F). The dried crystalline-monolayer nucleus (Figure 3F), formed on mica, was observed by an electron microscope, and a hexagonal 2D lattice structure has been directly proven. Two micrographs are shown in Figure 4. It is seen that the particle concentration around the empty places in the nucleus (Figure 4A) is less than that in the dense 2D crystal (Figure 4B) just at the nucleus boundary. The experimental results on glass were similar to those obtained on mica.

We also did experiments with much smaller latex particles of 55-nm diameter on mercury, mica, and glass. The pictures of the film thinning process resembled that

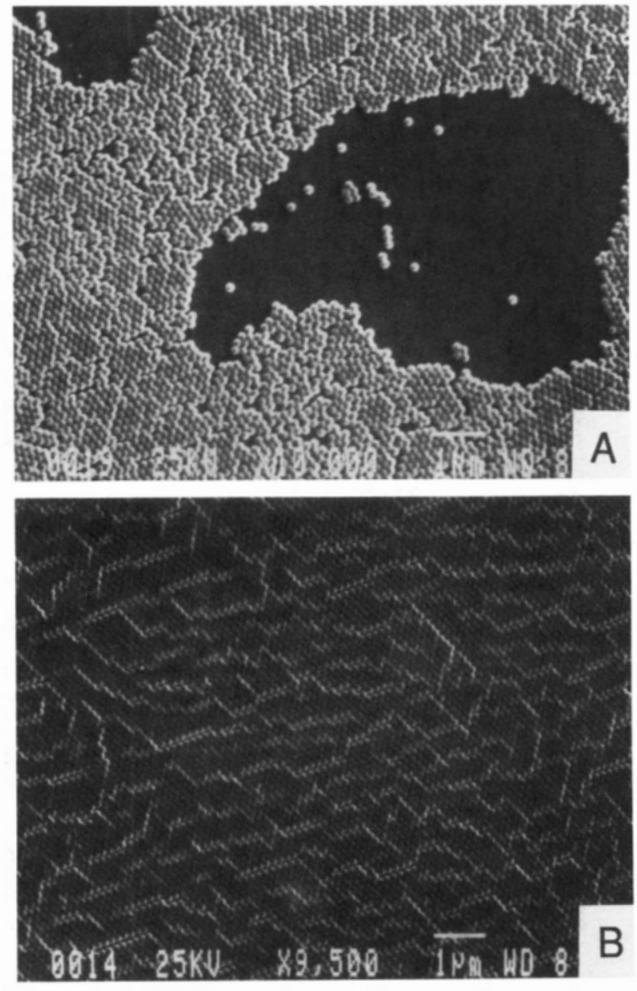

Figure 4. A SEM image of a crystalline-monolayer nucleus of 144 nm latex particles on glass: (A) two-dimensional-crystal domains around an empty place corresponding to one white spot in Figure 3F and (B) dense crystalline monolayer of hexagonal packing.

observed with 144-nm latex. However, the transition from a thin film to a monolayer nucleus on mercury was not observed. When the thickness of the film approached 90 nm, a transition from a primary to a secondary thin film was observed. A small spot with a thickness of about 30 nm appeared in the primary thin film. The spot did not contain particles and rapidly, for less than 1 s, expanded and occupied the entire film area. The expanding contact line pushed the particles toward the Gibbs–Plateau border. As a result a 2D nucleus did not usually form, although layers of particles were sometimes observed in the film near the contact line. Two stages of the nucleation on glass are shown in Figures 5A,B. The film containing 55-nm particles in a central area of Figure 5A is gray with a thickness of about 42 ± 15 nm. Two circular brighter spots are seen in the central part of the film in Figure 5A. They do not contain particles and represent concave water films with thicknesses smaller than the particle diameter. The spots expanded quickly and new ones also appeared during the nucleus formation. Finally, an ordered 2D nucleus was formed between the particle-free areas (Figure 5B). It was confirmed by the electron microscope observations that the crystal nucleus had hexagonal 2D lattice packing as shown in Figure 5C.

In Figure 6 we plotted as a function of time the results that were obtained for the film thicknesses of two samples of 55-nm latex on glass substrate and one sample of 144-

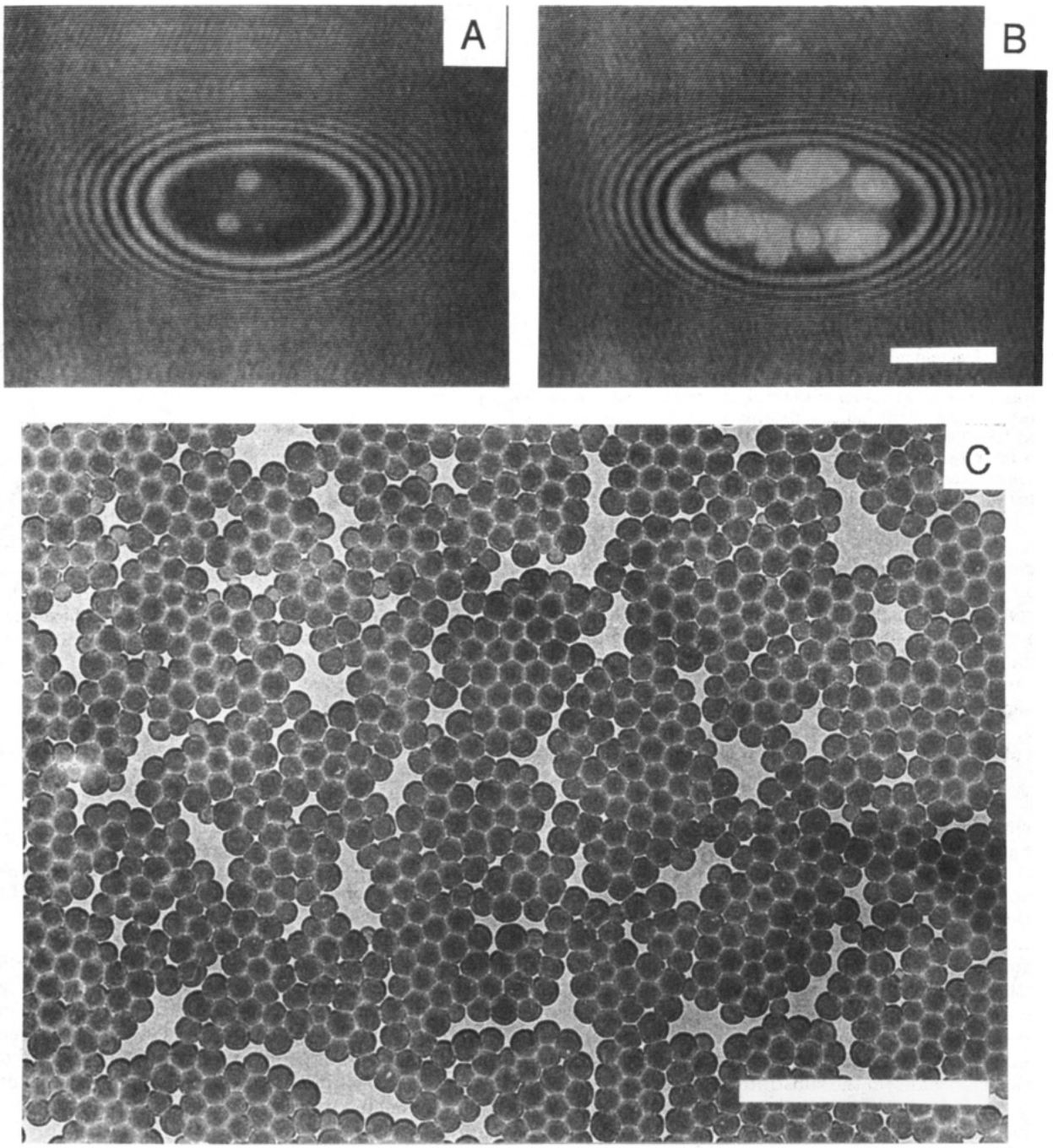

Figure 5. Suspension film containing latex particles of 55 nm diameter on glass: (A) formation of a thin film of thickness $h \approx 42 \pm 15$ nm, bright spots appear inside the film ($t = 56$ s); (B) drying of the formed crystalline-monolayer nucleus ($t = 59$ s). The bar is 100 μm. (C) TEM image of a crystalline monolayer of 55-nm latex particles on mica. The empty places between the structured domains may be due to the shrinking of particles after complete drying. The bar is 500 nm.

nm latex on mica. The moment when the nucleus was formed is shown with a small arrow on each curve in Figure 6.

Discussion

1. Wetting of the mercury surface was the principal problem in our experiments. To solve this problem, we use the results reported by Kaisheva[12] that sodium dodecyl sulfate (SDS) aqueous solution can form stable wetting films on negatively polarized mercury. He supposes that the sodium dodecyl sulfate molecules adsorb with the hydrophobic dodecyl sulfate tails against the mercury. In our experiments the sodium chloride added to the prewetting solution facilitates SDS adsorption. However, the prewetting solution high ionic strength causes precipitation of the latex suspension. To prevent this, we withdraw the prewetting solution from the crystallization cell and washed the mercury surface with deionized water before dropping the suspension. With the procedure proposed by us the adsorbed SDS monolayer remains at the mercury surface and keeps it wettable. Hence, we create conditions under which the mercury surface is wettable, the wetting film is stable, and the suspension does not precipitate.

2. Electrostatic Interactions between the Mercury Substrate and the Latex Particles. The latex particles in the original suspension are charged negatively, and hence, the nucleation must depend on the electrostatic interactions between the charged substrate and the particles. We control these interactions by varying the

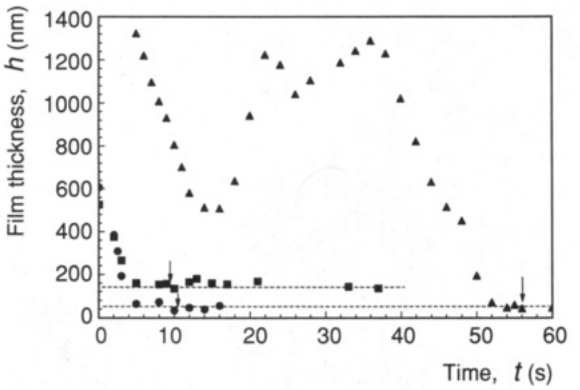

Figure 6. Dependence of the film thickness h on time t: (■) 144-nm latex on mica (the same sample as in Figure 3); (●) 55-nm latex on glass; (▲) 55-nm latex on glass (the same sample as in Figure 5). The arrows indicate the time when the nucleus was formed. The dashed lines correspond to the respective diameters of the latex particles. The instabilities of the film thickness between 400 and 1400 nm, which were observed with the sample denoted with (▲), did not disturb the nucleation at $h \approx 42 \pm 15$ nm.

electric potential applied to the mercury. Below we discuss the processes that were observed with micrometer-size latex particles in suspension films on mercury, when four different types of electric potentials were applied to the mercury.

Particles that are pressed toward a liquid interface can be assembled into ordered 2D domains by lateral capillary forces, immersion[9,10] or flotation.[13,14] The cause of both types of forces is the deformation of the liquid interface, which is supposed to be flat in the absence of particles. The larger the interfacial deformation, created by the particles, the stronger are the capillary forces. The cause of the interfacial deformation for the flotation forces is the resultant from gravity and the buoyancy force. The flotation force interaction energy between two 10-μm latex particles or smaller ones is less than kT (k is Boltzman constant and T is the absolute temperature).[13] Hence, in our experiments on mercury the flotation forces could not order the particles into domains at the upper film surface. The immersion forces can in principle enormously increase. However, when a 200-mV and above negative potential was applied to the mercury, the particles at the upper film surface distanced from the substrate. Hence, the immersion forces did not also order the particles at the upper film surface. Then, we supposed that the charged latex particles were lifted and pressed toward the upper film surface by the applied electric field. The arisen deformation of the upper film surface creates lateral capillary forces that can arrange charged particles into ordered 2D domains. We call these forces lateral *electro*capillary forces (see Figure 7A). Since the electrostatic repulsion is not as strong as the substrate reaction, the lateral electrocapillary forces are much weaker than the immersion forces that assemble the particles in a 2D array nucleus on a substrate. That is why the floating ordered domains were fragile and they were easily destroyed when the suspension was withdrawn from the cell.

At a negative potential of less than 200 mV, the electric field is not strong enough to push the particles against the water surface and they remain inside the suspension film.

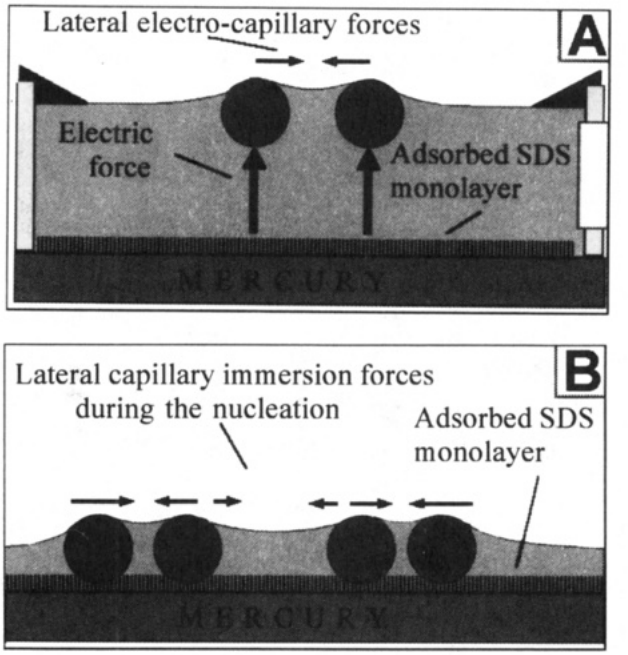

Figure 7. Location of micrometer-size particles in wetting films on mercury: (A) particles pushed toward the film surface by the electric field; (B) particles sandwiched between the upper film surface and the substrate.

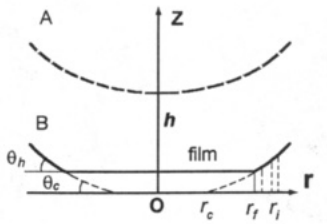

Figure 8. Sketch of the meniscus profile (A) before a plane-parallel film is formed and (B) after a plane-parallel thin film is formed. For notations see the Appendix.

However, the upper surface that presses micrometer-size particles to the mercury was curved (as shown in Figure 8A). The lateral forces that cause the particle depletion from the film are in fact immersion forces between a particle and a wall (capillary image forces).[13] Although weak in our experiments, the capillary image forces drove the micrometer-size particles into the bulk suspension, and thus a particle-free water film was formed. In the experiments with submicrometer-size particles a plane-parallel liquid film was formed before pressing the particles (see Figure 8B). The thickness of this film was greater than the particle diameter. When the film becomes thinner, a surface that is originally flat presses the particles to the substrate. The submicrometer-size particles, then, attract each other by the immersion forces also at an applied negative potential. The nucleation is the same as at an applied low positive potential, below 15 mV.

At a positive potential above 100 mV the SDS molecules desorb or change their orientation,[12] which makes mercury nonwettable. Then, the latex particles adsorb onto the mercury surface because of the electrostatic attraction and the entropy increase due to the water release from the hydrate atmospheres of the adsorbing latex particles. When the film on the mercury ruptures, the bumps of the latex particles are carried into the suspension bulk by the expanding contact line. We suppose that the forces that drive the particle bumps toward the cell wall are also capillary forces acting between a particle and a wall.[13]

(13) Paunov, V. N.; Kralchevsky, P. A.; Denkov, N. D.; Nagayama, K. *J. Colloid Interface Sci.* **1993**, *157*, 100.
(14) Chan, D. Y. C.; Henry, J. D.; White, L. R. *J. Colloid Interface Sci.* **1981**, *79*, 410.
(15) Kruglyakov, P. M. In *Thin Liquid Films: Fundamentals and Applications*; Ivanov, I. B., Ed.; Marcel Dekker: New York, 1988; p 778.

At a low positive potential between 3 and 15 mV the suspension film is stable, because the SDS molecules remain still adsorbed at the mercury/water interface. We suppose that the electric field drags the particles to the mercury surface and these attach lightly to the adsorbed SDS molecules (Figure 7B). When the micrometer-size latex particles are initially pressed by the curved upper film surface, the capillary forces that are caused by the inclination are weaker than the friction between the particles and the adsorbed SDS monolayer. The particles remain in the film and resist the local film thinning. Further withdrawing of the suspension leads to an appearance and increase of a uniformly flat film. When the film thickness decreases more, the immersion forces become stronger than the friction forces. Then, an ordered 2D nucleus starts to form.

3. Nucleation of a particle monolayer starts when the film thickness nearly equals the particle diameter. Initially the micrometer-size latex spheres on mercury are seen to have Brownian motion. The localizing of this motion means that the particles feel pressing by the upper film surface. The stronger the pressing, the smaller is the amplitude of the localizing motion. At some moment with the film thinning an attraction between the nearest particles starts (see Figure 7B). The nucleation starts from the film regions with greater particle concentration, because the capillary immersion forces are stronger between particles that are closer to each other.[9] The particle aggregation in the denser regions leads to particle consumption from the adjacent regions with smaller concentration. In the experiments on mercury the film thickness is controlled, the nucleation time is elongated, and the particles are packed in nuclei without open places, because of a particle influx from the Gibbs–Plateau border. In the experiments on solids, however, the film thickness is not controlled and the nucleation time is restricted by water evaporation from the film. The formation of open spots in the nuclei supports the hypothesis that, in the beginning of 2D-crystal nucleation, the capillary immersion forces rearrange the particles inside the film. Where the particle concentration is high, hexagonal lattice domains are formed, and where the particle concentration is low, particle-free spots appear (see, e.g., Figures 3E,F, 4A, and 5A,B). If the film thickness on solids is kept constant over time, as in the experiments on mercury, the open spots would be closed due to the lateral capillary forces between the already formed particle clusters and the particle influx from the suspension bulk. Therefore, the nucleus quality depends on the time of keeping constant film thickness. If this time is short the nucleus structure is similar to that shown in Figures 4A and 5C, where the monolayer density around the particle-free spots is less than that of the dense crystalline monolayer (Figure 4B).

4. Thickness of the Film from a Suspension of Submicrometer-Latex Particles. In the experiments with submicrometer latex particles, a plane-parallel liquid film is formed before the particles are pressed to the substrate by the upper film surface. On mercury the film thickness smoothly decreases, until the 144-nm particles are pressed, but does not smoothly decrease until the smaller 55-nm particles are pressed. This is due to the disjoining pressure, which arises and acts normally to the surfaces of thin liquid films (see, e.g., ref 15). In our experiments on mercury a transition from a primary to a secondary thin film is observed at thicknesses of about 90 nm. The transition starts with a narrow and sharp spot with a thickness of 30 nm. It appears randomly in the primary thin film of the suspension of 55-nm particles. The contact line separating the primary and secondary thin films, then, expands rapidly and pushes all the particles into the Gibbs–Plateau border.

On glass and mica substrates the suspension film thickness smoothly decreases to thicknesses of less than 40 nm. As a result, nuclei of monolayers from particles with both diameters, 144 and 55 nm, start to form when the film thickness becomes equal to the particle diameter (see Figure 6). The hydrodynamic instabilities of the film thickness as those observed between 400 and 1400 nm for the sample denoted with triangles (▲) do not disturb the nucleation, when it proceeds at a smaller thickness, $h \approx 42 \pm 15$ nm for the same sample. Figure 6 confirms the importance of the film thickness for the crystalline-monolayer nucleation, which is due to the action of the immersion forces.

Conclusions

We studied the nucleation of 2D crystals from latex particles in liquid films on mercury, glass, and mica. In the experiments on mercury we controlled the thickness of the suspension film inside the cell and the electric potential applied to the mercury. We detected three steps of the nucleus formation. In the first step the nucleation started with a redistribution of the particles inside the film when the thickness of the film became equal to or less than the particle diameter. Domains of an ordered phase then appeared. In the second step these domains attracted each other and formed the nucleus. The nucleus annealing is the third step of the nucleus formation.

With the submicrometer particle suspensions, formation of a thin film preceded the particle aggregation. The computations showed that monolayer nuclei started to form when the film thickness became equal to or less than the particle diameter. The monolayers from 55-nm latex particles on mercury did not nucleate because the suspension film thicknesses in the range between 30 and 90 nm were not stable under those experimental conditions. The particle-free places on solids resulted from the immersion force action in the first nucleation step. In these experiments the second and third nucleation steps were skipped because of the nucleus rapidly drying.

Our study suggests that hexagonally-packed latex particle 2D-crystal nuclei on substrates are arranged by the immersion capillary force[9,10] action. The introduced lateral electrocapillary forces associated particles into ordered 2D domains on the upper surface of thick films on mercury.

Acknowledgment. This work was supported financially by the ERATO Program of the Research and Development Corporation of Japan (JRDC). We are thankful to our colleagues Mrs. M. Yamaki for SEM analyses of the samples, Mr. G. S. Lazarov for preparation of the graphics, and Dr. G. Picard for valuable discussions on preparation of this paper.

Appendix

Computation of the Film Thickness from the Newton Interference Rings. A sketch of the film and the adjacent meniscus in the experimental cell is presented in Figure 8. Initially the meniscus is concave with a distance h between the apex and the substrate (Figure 8A). When the water/air surface starts to interact with the substrate, a thin liquid film of thickness h forms (Figure 8B). The shape of the meniscus profile, $z(r)$, satisfies the

Laplace equation of capillarity written as a set of two equations as follows:

$$\frac{dr \sin\theta}{r\,dr} = \frac{P_c}{\sigma} \quad (1)$$

$$\frac{dz}{dr} = \sin\theta \quad (2)$$

Here, a negligible gravity term and a small meniscus slope ($\tan\theta \approx \sin\theta$) are assumed, r is the radial coordinate, $\theta(r)$ is the running slope angle, σ is the surface tension of the solution, and P_c is the capillary pressure. When a thin film is formed (Figure 8B), there is a small transition region between the film surface and the meniscus. The shape of the water surface in this region does not satisfy the above set of two equations. Nevertheless, one can extrapolate the meniscus (the surface which satisfies the Laplace equation) into the film until it intersects the substrate surface along the contact line of radius r_c. The angle formed between the extrapolated Laplace surface and the plane of the substrate is called the contact angle, θ_c. One can also define another contact angle, θ_h, at the intersection between the extrapolated meniscus and the plane of the film surface. The radius of the intersection contact line, r_f, is experimentally measured. It coincides with the film radius of uniform reflected light intensity. The variables r_i (i = 1, 2, 3, ...) are the radii of the interference fringes (see Figures 3, 5, and 8), representing minimum or maximum intensity, which are due to the interference of the light reflected from the upper (water) surface and that from the lower (substrate) surface. The values of r_i measured by optical observation have an accuracy of 0.5–2.5 μm depending on the meniscus slope. From the measured r_i one can reconstruct the shape of the meniscus by varying three parameters: θ_c, r_c, and P_c.[16] Here we outline the computation of the film thickness, h, based on the results from ref 16.

By integration of eq 1, one obtains the following equation:

$$\sin\theta = \frac{P_c}{2\sigma}\left(r - \frac{r_k^2}{r}\right) + \frac{r_c}{r}\sin\theta_c \quad (3)$$

Hence, for the meniscus profile in the Gibbs–Plateau border one derives by integration of eq 2 the following equation:

$$z(r) = \frac{P_c}{2\sigma}\left[\frac{r^2 - r_c^2}{2} - r_c^2 \ln\frac{r}{r_c}\right] + r_c \sin\theta_c \ln\frac{r}{r_c} + z_c \quad (4)$$

Here, z_c is a constant of integration, $z_c = z(r_c)$. The film thickness, h, follows from eq 4 at $r = r_f$, as shown by eq 5. The error of the film thickness calculation, Δh, depends

$$h = z(r_f) \quad (5)$$

on the experimental error, Δr_f, in determination of the film radius, r_f, according to eq 6. The magnitude of Δh is

$$\Delta h = \tan\theta_h \, \Delta r_f \quad (6)$$

a criterium for applicability of the computational procedure. For example, when the contact angle is large, Δh is also large and the numerical results contain large error. The contact angle, θ_h, is calculated by eq 3. Usually z_c in eq 4 is zero, except for some relatively thick films where z_c is not zero (i.e., the extrapolated meniscus profile does not intersect the plane $z = 0$).[17]

When a plane-parallel thin film is still not formed (as in Figure 8A), h is calculated by integration of eqs 1 and 2 at the boundary condition as follows:

$$\theta(r=0) = 0 \quad (7)$$

The capillary pressure, P_c, the contact angle, θ_c, the contact radius, r_c, and the film thickness, h, are calculated by minimizing the dispersion between the positions of the Newton fringes obtained experimentally and the positions calculated by integration of the Laplace equation (see ref 16 for the general approach).

For all data which are reported in this study, the film thickness was calculated without taking into account that the refractive index of the suspension near the contact line was little higher than the suspension refractive index in the bulk, which was due to the variation of the particle concentration. For example, the thickness of the film shown in Figure 3C was calculated to be 148 ± 20 nm (greater than the particle diameter, 144 nm). If one supposes that the latex particle concentration in the Gibbs–Plateau border increased to 30 vol %, recalculation would give a film thickness of 139 ± 20 nm, which is less than the particle diameter. Due to the evaporation of water from the film and to the water flux carrying particles toward the contact line, the particle concentration in the vicinity of the film periphery can be even higher than 30 vol %.

(16) Dimitrov, A. S.; Kralchevsky, P. A.; Nikolov, A. D.; Wasan, D. T. *Colloids Surf.* **1990**, *47*, 299.

(17) Martynov, A. G.; Ivanov, I. B.; Toshev, B. V. *Kolloidn. Zh.* **1976**, *38*, 474.